

Dynamic Matching Markets in Power Systems: Concepts and Solution using Deep Reinforcement Learning

Majid Majidi*, *Student Member, IEEE*, Deepan Muthirayan*, *Member, IEEE*, Masood Parvania, *Senior Member, IEEE*, Pramod P. Khargonekar, *Fellow, IEEE*

Abstract—Traditional bulk load flexibility options, such as load shifting and load curtailment, for managing uncertainty in power markets limit the diversity of options and ignore the preferences of the individual loads, thus reducing efficiency and welfare. This paper proposes an alternative to bulk load flexibility options for managing uncertainty in power markets: a reinforcement learning based dynamic matching framework. More specifically, a novel hybrid learning model is proposed for determining the matching policy that is a composition of a fixed rule-based function and a trainable component that can be trained by matching data with no prior knowledge or expert supervision. The output of the trainable component is a probability distribution over the matching decisions for the individual customers. The proposed hybrid learning model enables the learning algorithm to find an effective matching policy and simultaneously satisfy the load servicing constraints. The simulations show that the proposed learning algorithm learns an effective matching policy for different generation-consumption profiles and exhibits better performance compared to standard online matching heuristics such as Match on Arrival, Match to the Highest, and Match to the Earliest Deadline policies.

Index Terms—Dynamic matching markets, power systems, reinforcement learning, policy gradient.

I. INTRODUCTION

LARGE scale integration of renewable energy sources (RES) into the power systems is a major strategy for the decarbonization of the energy system. RES include combinations of utility-scale centralized and distributed wind and solar power plants. Integration of RES in the operation and control of the grid is a significant challenge because photovoltaic (PV) solar and wind are highly uncertain, inherently variable, and largely uncontrollable. The flexibility of loads represent a promising solution to manage the uncertainty in RES and thereby achieve greater penetration of RES [20]. The challenge here is the scheduling and matching of uncertain supply to the uncertain flexible load [1].

This work is supported in part by the National Science Foundation under Grant ECCS-1839429.

M. Majidi and M. Parvania are with the Department of Electrical and Computer Engineering, The University of Utah (emails: majid.majidi@utah.edu, masood.parvania@utah.edu).

D. Muthirayan and P. P. Khargonekar are with the Department of Electrical Engineering and Computer Sciences, University of California Irvine, Irvine (emails: deepan.m@uci.edu, pramod.khargonekar@uci.edu). *Both authors made equal contribution.

A. Contribution

This paper proposes a dynamic matching market and solution using Deep Reinforcement Learning (DRL) to match the random supply and load flexibility in power systems, whose objective is to maximize social welfare subject to customized servicing of loads using RES. Traditionally, the power markets were managed using bulk load flexibility options such as load shifting and load curtailment, supplied by aggregators to the system operator, to manage the uncertainty of the real-time market [2], [7], [18]. The drawback of the bulk load flexibility options is that (i) it limits the diversity of options that is available for the system operator by pooling the resources together in bulk and (ii) does not take into account the preferences of individual flexible loads. To address these limitations, the proposed dynamic matching market solution treats every individual supply entity and flexible demand as an independent resource and matches them while satisfying their constraints and preferences and accounting for future uncertainty.

Matching in dynamic markets is a particularly challenging problem when there is uncertainty about the future. Online matching has been extensively studied both in adversarial and stochastic settings in a variety of application domains [9]–[14]. These papers explore and analyze matching algorithms and provide lower bound guarantees for their performance. While online matching heuristics suggested in [9]–[14] have provable lower bound guarantees, the recent successes of machine learning in various applications suggests the possibility that a learning approach could offer a powerful alternative for designing matching policies for new conditions. Therefore, the dynamic matching market proposed in this paper provide a DRL framework for learning the online matching policy without prior knowledge or supervision. The primary advantage of the proposed learning approach is that it provides a flexible and adaptable approach to find an effective matching strategy for any new scenario with just raw load and generation data and no prior experience or expert supervision or elaborate design. This is demonstrated in the numerical results in Section V by showing that the proposed learning approach is able to learn an effective strategy for a wide range of generation-consumption profiles.

In summary, the key contribution of the paper is a trainable matching policy for dynamic matching markets that: a) enables the learning algorithm to learn an effective matching policy,

b) satisfies the individual load servicing constraint, and c) addresses the exponential scaling of the action space for the matching problem, which is a standard challenge for DRL algorithms [15]. Another contribution is the derivation of the policy gradient reinforcement learning algorithm for the proposed policy. The numerical results provides a detailed comparison of the learning algorithm with three other baseline online matching algorithms, demonstrating that the proposed algorithm achieves the highest average social welfare across the different generation-consumption profiles.

B. Related Work

There is a large body of work related to operation of distributed energy resources and flexible loads [16]–[24]. Authors in [16]–[20] propose and study different algorithms for flexible loads and RES scheduling with the objective of minimizing the operation cost. The work in [21] provides asymptotic performance guarantees for an approach based on online stochastic optimization, while [22] provides a theoretical analysis for a real-time algorithm for the objective of minimizing operational costs. The work in [23] develops a model for balancing flexible loads and local generation, and discuss its game theoretic properties. Authors in [24] propose a model predictive control scheme for minimizing customer dissatisfaction plus generation cost. All of these works develop optimization based approaches that require prior knowledge of the market scenario model (see below).

RL is extensively studied by researchers from many fields such as artificial intelligence (AI), control, operations research, and economics, resulting in many books published on the topic [25]–[27]. Recent success of combining RL and Deep Neural Networks (DNNs) [28], [29], has given rise to the field of Deep Reinforcement Learning (DRL). Many subsequent works on DRL have significantly advanced the field [30]–[36]. The matching problem is challenging because (i) the action space is exponential in the number of customers, (ii) the matching policy has to satisfy the load servicing constraints (system constraints that should never or rarely be violated is typically a challenge in RL [15]), and (iii) the learning algorithm should converge to an effective solution; RL algorithms can converge to a local optimum [15]. The contribution here is proposing a reinforcement learning framework that addresses the aforementioned challenges for the matching problem.

II. MATCHING MARKET SETTING

This section describes the matching market setting: the supply model, the demand model, the scenario model for the power market and then the matching problem and how the performance of the market is evaluated.

A. Energy Resources Model

We consider two sources of supply for the dynamic matching market: 1) upstream grid supply (type gs), and 2) distributed renewable energy sources (D-RES) (type rs). We assume that upstream grid supply, denoted by $p_t \in \mathbb{R}$, is sufficiently large and that it is priced at c/kWh , the retail

price of electricity. The D-RES, such as PV solar and wind generation, are by nature variable and uncertain, and their availability depends on weather, e.g., solar irradiance, wind speed. We denote the D-RES generated at time t by $r_t \in \mathbb{R}$. The unit cost of renewable units is assumed to be zero.

B. Flexible Load Model

Each load (or customer) is characterized by three parameters, $\{a^i, q^i, d^i\}$, where $a^i \in \mathbb{N}$ is the arrival time of the customer, $q^i \in \mathbb{R}$ is the load requested by the customer, and $d^i \in \mathbb{N}$ is the deadline by which the customer is to be served. The heterogeneity of customers lies in the differing deadlines (also their criticality). When customer i arrives at the platform it reports its load request q^i and its service deadline d^i . This paper assumes that the customers report truthfully on arrival. The utility function of a customer, denoted by π_t^i , represents the customer's willingness to pay for a unit of energy, and is defined as follows:

$$\begin{aligned} \pi_t^i &= c - b^i(t - a^i), \quad \pi_t^i \geq 0, \quad \forall t, \quad a^i \leq t \leq d^i, \\ b^i &= c/(d^i - a^i), \end{aligned} \quad (1)$$

where b^i is determined by the criticality of the customers, which is the percentage of drop in the willingness to pay from their arrival time to their deadline. If the criticality of the customers is 100% then their willingness to pay is zero at their deadline, but their slope b^i depends on their respective deadlines. This models the fact that the customers' satisfaction typically decreases with delay.

In (1), customer's willingness to pay is less than or equal to the grid supply price c/kWh . This is reasonable considering that the grid supply is available at this price at all times. The novelty of our modeling is the fact that the customers' willingness to pay decay with time and at distinct rates. We denote the number of customers who arrive on the platform at time t by $n_t \in \mathbb{N}$, which is upper bounded by \bar{n} .

C. Market Scenario Model

Let $z_t := [a_t^\top, q_t^\top, d_t^\top, r_t]^\top$, where $a_t \in \mathbb{N}^{\bar{n}}$ is the vector of the arrival times of the customers which arrive at time t , $q_t \in \mathbb{N}^{\bar{n}}$ is the vector of their respective requested loads, $d_t \in \mathbb{N}^{\bar{n}}$ is the vector of their respective deadlines, and $r_t \in \mathbb{R}$ is the amount of renewable generation at time t . The scenario at time t is given by:

$$Z_t^\top = [z_1^\top, z_2^\top, \dots, z_{t-1}^\top, z_t^\top]$$

The probability that $z_t = z$ is given by the stochastic process modeled by $\mathbb{P}(z_t = z | Z_{t-1})$. This process is not known to the market operator. Let $x_t := [a_t^\top, q_t^\top, d_t^\top, q_{p,t}^\top, r_t]^\top$, where $q_{p,t}$ denotes the vector of the portion of the requested loads that has not been served to the customers who arrived at t . Then the state of the market, $X_t \in \Omega_t$, is given by:

$$X_t^\top = [x_1^\top, x_2^\top, \dots, x_{t-1}^\top, x_t^\top].$$

Note that state X_t depends on the scenario Z_t and the matching decisions till time $t - 1$.

¹ $[\cdot]^\top$ denote the matrix transpose operation.

D. Dynamic Matching Problem

The proposed dynamic matching market of the power system operates for a duration of T within an epoch with time periods spaced equally at an interval Δt . The loads arrive in a sequential fashion and the generation of D-RES are governed by the stochastic process described in Section II-C. At instant t , the market operator can decide to match the energy demands of the loads that are currently active for the increment of time Δt to D-RES or the grid supply or wait till later to match it.

Denote the set of all the customers active on the platform at time t by A_t . Denote the set of supply types by $S_t = \{gs, rs\}$. It follows that A_t is a function of X_t . Let q_p^i denote the portion of the requested load by customer i that has not been served. Denote the amount of supply of type j matched to customer i at time t by $M_t(j, i, X_t) \in \mathbb{R}$.

The market operator has the following information to make its matching decisions at time t : the set of active customers A_t , their arrival time and deadlines, the amount of renewable generation r_t , customers active before t and renewable generation for each time step before t . Let c_j denote the unit cost of type j supply. The dynamic matching problem (2) for the market operator is maximizing social welfare under the above information setting subject to the load and supply constraints:

$$\begin{aligned} \sup_{M_t} \sum_{t=1}^T \sum_{i \in A_t} \sum_{j \in S_t} (\pi_t^i - c_j) M_t(j, i, X_t), \text{ s.t.} \\ \sum_{j \in S_t} M_t(j, i, X_t) \leq q_p^i, \quad \forall i \in A_t, \quad \sum_{i \in A_t} M_t(rs, i, X_t) \leq r_t, \end{aligned} \quad (2)$$

where the dependency of M_t on X_t accounts for the dependency of the matching decision on the full state information. The problem as stated is an online matching problem because at any point of time t during the operation of the market the market operator can only make its matching decision based on the information of the current and the past customers and supply quantities and with uncertainty on the future.

E. Performance Metric for a Matching Policy

The performance measure for a general online matching policy, χ (whose policy for time t is denoted by $\chi_t(\cdot, \cdot, \cdot)$), deployed by the market operator is

$$\begin{aligned} W[\chi] &= \sum_{t=1}^T \sum_{i \in A_t} \sum_{j \in S_t} (\pi_t^i - c_j) M_t(j, i, X_t), \\ M_t(j, i, X_t) &= \chi_k(j, i, X_t), \end{aligned}$$

which equals the social welfare achieved by the algorithm M for the duration T of the market.

III. REINFORCEMENT LEARNING FRAMEWORK

Here we propose a learning framework that consists of (i) a trainable matching policy and (ii) a reinforcement learning algorithm to train the policy from the load and generation data for multiple instances (multiple epochs) of the market. The proposed reinforcement learning algorithm is a policy gradient algorithm that trains the matching policy from customer and

D-RES data by evaluating its own performance. Thus, the proposed training procedure does not require supervision or expert knowledge. Next, we first briefly discuss the structure of the matching policy and then discuss the learning algorithm. We denote the expectation with respect to all sources of randomness by $\mathbb{E}[\cdot]$.

A. General Matching Policy

Recall that the general online matching policy is denoted by $\chi = \{\chi_1, \chi_2, \chi_3, \dots, \chi_T\}$, where χ_t is the policy for time t . Let us denote the space of matching at time t by \mathcal{M}_t , where each member of this set is a feasible matching for a state that can be realized at time t . For any $m \in \mathcal{M}_t$, the component that specifies whether a customer i at t is matched to supply type j , $m_{j,i} \in \{0, 1\}$, where one denotes ‘‘matched’’ and zero denotes ‘‘not matched’’. Then a general matching policy χ_t is given by:

$$\chi_t : \Omega_t \rightarrow \mathcal{M}_t.$$

B. Model of Matching Policy

We propose a certain structure for the matching policy χ_t , which has a learnable component and a fixed component. The fixed component accounts for the fact that the customers have to be matched before their deadline and that the matching to renewable generation cannot exceed the amount that is generated. The learnable component is the policy μ_t . The policy μ_t outputs the probability of matching a load without specifying which type of supply to match to. This simplifies the learnable part of the matching policy, whose size would otherwise scale exponentially with the number of customers. Denote the space of such matching decisions for time t by \mathcal{H}_t . For any $m \in \mathcal{H}_t$, the component that corresponds to customer i , $m_i \in \{0, 1\}$, where zero denotes ‘‘not to be matched’’ and one denotes ‘‘to be matched’’. We denote the space of probability measures over the set \mathcal{H}_t by $\mathcal{P}_{\mathcal{H}_t}$. Then, the policy μ_t is given by:

$$\mu_t : \Omega_t \rightarrow \mathcal{P}_{\mathcal{H}_t}.$$

Let $m_t \in \mathcal{H}_t$ be given by $m_t \sim \mu_t$. We denote the component of m_t that corresponds to customer i by $m_{t,i}$, where $m_{t,i} \in \{0, 1\}$. The output m_k is input to a second function, φ , which matches the customers for whom $m_{t,i} = 1$ and up to r_t of them to the renewable units. It matches any remaining customer for whom $m_{t,i} = 1$ to the grid supply. If $\sum_i q_i m_{t,i} < r_t$ then in addition to the above step it matches the remaining $r_t - \sum_i q_i m_{t,i}$ to available customers. This function is the key function that influences the learning algorithm to converge to an effective solution. The function φ is given by:

$$\varphi : \mathbb{R} \times \mathcal{H}_t \rightarrow \mathcal{M}_t.$$

Denote the component of φ that specifies whether customer i is matched to supply type j by $\varphi_{j,i}$. The output of φ is input to a third function, ν , that overturns the decision to not to match the customers with immediate deadline:

$$\nu_{j,i} = \begin{cases} 1 & \text{if } d^i = t, \text{ } i \text{ is active, } \varphi_{rs,i} = \varphi_{gs,i} = 0 \\ & \text{and } j = \text{gs,} \\ \varphi_{j,i} & \text{otherwise.} \end{cases}$$

The function ν ensures that the constraint that the loads should be served by their deadline is always satisfied. Thus, the overall matching policy for time t , χ_t , is given by:

$$\chi_t = \nu \circ \varphi \circ m_t, m_t \sim \mu_t. \quad (3)$$

Let μ_t to be parameterized by θ_t and denote the parameterization by $\mu_t(\cdot; \theta_t)$. Later we discuss the parametric model for μ , $\mu = \{\mu_1, \mu_2, \mu_3, \dots, \mu_T\}$. The learning algorithm trains the parameter θ_t for every t using the load and generation data by evaluating its own performance.

Let $X = \{X_1, X_2, X_3, \dots, X_T\}$. We use $X \sim \mu$ as shorthand notation to denote the dependence of the state on the random policy μ . Given the performance metric for the matching policy, the value function for the policy χ , V_χ , is the expected welfare for the duration T of the market. Thus:

$$V_\chi = \mathbb{E}_{X \sim \mu} [W[\chi]] \text{ where} \\ W[\chi] = \sum_{t=0}^T \sum_j \sum_{i \in A_t} (\pi_t^i - c_j) \chi_{t,j,i}(X_t). \quad (4)$$

C. Policy Gradient Algorithm

We use $\mathbb{E}_{X_t \sim \mathbb{P}_t(\cdot)}$ as a shorthand for expectation over $X_t \sim \mathbb{P}(\cdot | X_{t-1}, \chi_{t-1})$, where $\mathbb{P}(\cdot | X_{t-1}, \chi_{t-1})$ denotes the transition probability from state X_{t-1} under the policy χ_{t-1} . Let $m_{t:T} = \{m_t, m_{t+1}, \dots, m_T\}$, $\mu_{l:T} = \{\mu_t, \mu_{t+1}, \dots, \mu_T\}$. Let

$$V_{t+}^\chi(X_{t+1}) := \mathbb{E}_{m \sim \mu} \sum_{l=t+1}^T \left[\sum_j [(\pi_l(A_l) - c_j)^\top \chi_{l,j,A_l}] \right], \\ = \mathbb{E}_{m_{t+1:T} \sim \mu_{t+1:T}} \sum_{l=t+1}^T \left[\sum_j [(\pi_l(A_l) - c_j)^\top \chi_{l,j,A_l}] \right],$$

where $(\pi_l(A_l) - c_j)^\top \chi_{l,j,A_l}$ is the shorthand for $\sum_{i \in A_t} (\pi_t^i - c_j) \chi_{t,j,i}(X_t)$. Let:

$$v_t^\chi := \sum_j [(\pi_k(A_t) - c_j)^\top \chi_{k,j,A_t}(X_t)], \\ V_t^\chi(X_t) := \mathbb{E}_{m_t \sim \mu_t} [V_{t+}^\chi(X_{t+1})], \quad (5)$$

where, $V_t^\chi(X_t | m_t) := v_t^\chi + \mathbb{E}_{X_{t+1} \sim \mathbb{P}_{t+1}(\cdot)} [V_{t+}^\chi(X_{t+1})]$. Then, from the definition of V_χ it follows that:

$$\frac{\partial V_\chi}{\partial \theta_t} = \mathbb{E}_{X_t} \left[\frac{\partial V_t^\chi(X_t)}{\partial \theta_t} \right].$$

Then, from the definition of $V_t^\chi(X_t)$ it follows that:

$$\frac{\partial V_\chi}{\partial \theta_t} = \mathbb{E}_{X_t} \sum_{m_t \in \mathcal{H}_t} \frac{\partial \mu_t(m_t; \theta_t)}{\partial \theta_t} [v_t^\chi \\ + \mathbb{E}_{X_{t+1} \sim \mathbb{P}_{t+1}(\cdot)} V_{t+}^\chi(X_{t+1})].$$

We can rewrite the above equation as:

$$\frac{\partial V_\chi}{\partial \theta_t} = \mathbb{E}_{X_t, m_t \sim \mu_t} \left[\frac{\partial \log \mu_t(m_t; \theta_t)}{\partial \theta_t} V_t^\chi(X_t | m_t) \right]. \quad (6)$$

The previous equation gives the gradient of the value function w.r.t the policy parameter θ_t . An unbiased estimate of the gradient in (6) is:

$$\delta_t^\theta = \left[\frac{\partial \log \mu_t(m_t; \theta_t)}{\partial \theta_t} V_t^\chi(X_t | m_t) \right]. \quad (7)$$

The gradient in (7) is not computable because $V_t^\chi(X_t | m_t)$ is unknown. In place of $V_t^\chi(X_t | m_t)$, we can use the social welfare from t to T for a sample epoch under the policy χ :

$$\delta_{t,r}^\theta = \frac{\partial \log \mu_t(m_t; \theta_t)}{\partial \theta_t} \left[\sum_{l=t}^T v_l^\chi \right]. \quad (8)$$

This gradient is computable using the data from a sample epoch ($Z = \{Z_1, Z_2, \dots, Z_T\}$) and the matching decisions as determined by the policy χ for this sample epoch. Additionally the gradient estimate is also unbiased because

$$\frac{\partial V_\chi}{\partial \theta_t} = \mathbb{E}[\delta_{t,r}^\theta].$$

The vanilla policy gradient learning algorithm learns the policy parameter for each time step by the following stochastic gradient ascent algorithm:

$$\theta_t \leftarrow \theta_t + \gamma_\theta \delta_{t,r}^\theta, \quad (9)$$

that iteratively updates θ_t by using the computed gradient $\delta_{t,r}^\theta$ for multiple sample epochs, one every update step.

We also propose a second learning algorithm, called the actor-critic algorithm AC- k . This algorithm, in addition to learning the matching policy μ also learns an approximation of the value function $V_t^\chi(X_t)$ called the critic function. The critic function is parameterized by ϕ_k and is denoted by $V_k^\chi(X_k; \phi_k)$. The approximate policy gradient for the actor-critic algorithm AC- k is given by:

$$\delta_{t,k}^\theta = \frac{\partial \log \mu_t(m_t; \theta_t)}{\partial \theta_t} \left[\sum_{l=t}^{t+k-1} v_l^\chi + V_{t+k}^\chi(X_{t+k}; \phi_{t+k}) \right]. \quad (10)$$

The actor-critic algorithm (AC- k) learns the policy parameters by the following stochastic gradient ascent algorithm:

$$\theta_t \leftarrow \theta_t + \gamma_\theta \delta_{t,k}^\theta. \quad (11)$$

The parameter ϕ_k of the critic function is similarly learnt by stochastic gradient descent for its least-squares error:

$$\phi_k \leftarrow \phi_k - \gamma_\phi \left(V_k^\chi(\cdot; \phi_k) - \sum_{l=k}^T v_l^\chi \right). \quad (12)$$

The complete algorithm is given in Algorithm 1. The algorithm uses the ADAM gradient algorithm [37] of the gradient updates in (11) and (12).

IV. NEURAL NETWORK MODEL

The proposed parametric model for the learnable component μ is a Temporal Convolution Network (TCN) [38], whose weights are collectively denoted by θ . Temporal Convolution Networks use 1D fully-causal convolutional network (FCN) architecture (see Fig. 1). TCNs are specified by (i) the number of input channels, (ii) the number of layers or blocks, (iii) the number of filters (similar to the number of filters in Convolutional Neural Networks (CNNs)), (iv) the filter size, and (v) the dilation factor for each layer or block. In Fig. 1, the number of input channels is one, the number of filters or convolution operations is one for each layer (where the different filters are color coded differently), the number of

Algorithm 1: Actor-Critic (AC- k) Policy Gradient Learning Algorithm

- 1) Initialize $\mathcal{D} = \emptyset$, $j = 0$
 - 2) Initialize $\theta_k \forall k \in [1, \dots, T]$. N : number of epochs
 - 3) for $i = 1 : N$
 - a) $j = j + 1$
 - b) Set $D_i = \{\{X_k, m_k, v_k^x\} \forall k \in [1, \dots, T]\}$
 - c) Include D_i into \mathcal{D}
 - d) if $j == M$

Update θ_k by ADAM of Eq. (11) using \mathcal{D}

Update ϕ_k by ADAM of Eq. (12) using \mathcal{D}

$j = 0$; $\mathcal{D} = \emptyset$

end
 - end
 - 4) end
-

inputs for each filter operation or the filter size is two, the dilation factor varies by layers and in each subsequent layer the dilation factor is doubled.

A simple causal convolution can only look back at history of size that is linear with the depth of the network. This makes it challenging to apply simple causal convolutions on sequence tasks. The use of dilation in the upper layers allows the architecture to look back at history of size that is exponential in the depth of the network, making the model efficient. The inclusion of residual connections enable the construction of deep networks as in CNNs. Each filter of a TCN corresponds to the kernel of the convolution operation it corresponds to and each convolution operation is 1D (convolution over the time dimension). Within each layer or block there can be multiple sub-layers of causal convolution layers (see Fig. 2). Instance Normalization [39] and Spatial Dropout [40] can also be included in each layer (or block). Normalization is a standard technique to improve the speed of convergence and dropout is a widely used technique to regularize models in deep learning.

Just as in a recurrent neural network (RNN), the output of a hidden layer is computed by applying the filters of a layer repeatedly by shifting them by a stride of one over the sequence produced by the previous layer (see Fig. 1). Causality is achieved by ensuring the inputs to the filter from the input sequence are limited to the step in the output sequence of the layer for which the output is being calculated (see Fig. 1).

Temporal convolution networks have several advantages. Firstly, TCNs can model input lengths of variable size just like RNNs. TCNs do not have the problem of exploding or vanishing gradients that RNNs have because the backpropagation path in TCNs is different from the temporal direction. TCNs, by their very construction, are very flexible models because they provide multiple ways to expand the receptive field, for eg., either by using larger dilation, or adding additional layers, or just by increasing the size of the kernel filters. Additionally, computation is efficient in TCNs because convolutions in an individual layer are parallelizable. Thus, TCNs combine the best aspects of both RNNs and CNNs and are highly effective at modeling sequential data.

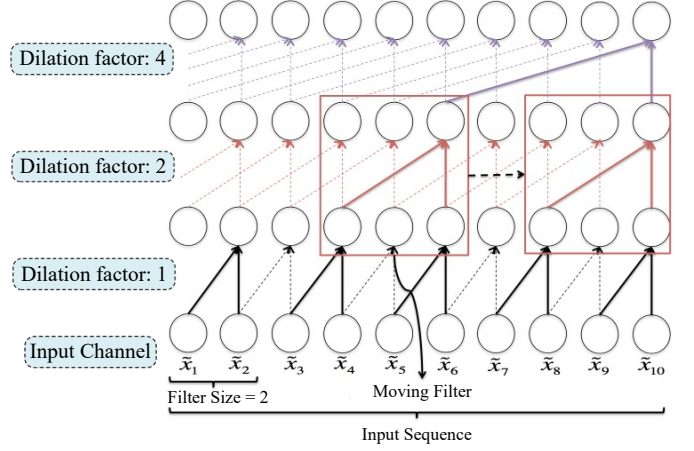


Fig. 1: Temporal Convolution Network.

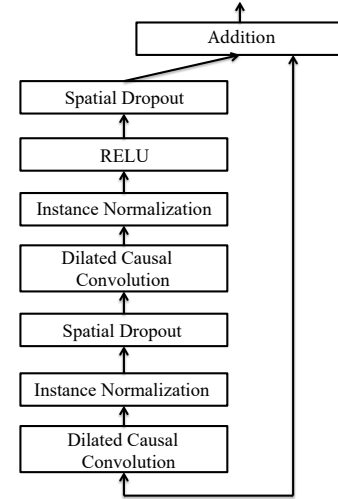


Fig. 2: A Single Block of TCN.

A. TCN Model for μ

Let the TCN corresponding to μ be functionally denoted by TCN_μ . Let $\tilde{x}_t = [q_t^\top, d_t^\top, q_{p,t}^\top, r_t]$. Let $\tilde{X}_t^\top = [\tilde{x}_1^\top, \tilde{x}_2^\top, \tilde{x}_3^\top, \dots, \tilde{x}_t^\top]$. For each time step t , the input to the TCN is \tilde{X}_t and the output of TCN is the individual probabilities that the respective customers will be matched. Let the vector of probabilities that the customers will be matched be given by $P_\mu^m \in [0, 1]^{\bar{n} \times T}$. Then:

$$P_\mu^m = \text{TCN}_\mu(\tilde{X}_t).$$

The input \tilde{X}_t is fed to the TCN model as shown in Fig. 1, i.e. the input \tilde{X}_t is fed to the NN as the sequence $\{\tilde{x}_1, \tilde{x}_2, \tilde{x}_3, \dots, \tilde{x}_t\}$. Clearly for this setting, the number of input channels is equal to the size of \tilde{x}_k for any k , which is equal to $\bar{n} \times 3 + 1$. The exact specification of the filter size, the number of filters, the number of layers or blocks are discussed later in the results section. The dilation factor is increased by two for every subsequent layer.

The output of the TCN model is of a fixed size for each time step t . The size is the maximum number of customers that can be active at any point of time, which is equal to $\bar{n} \times T$. While reading the output of the TCN model at time step t , the

values of probability of matching corresponding to the active customers are read. Denote the probability of matching for the active customer i at time step t by $P_{\mu,i}^m$. The distribution μ_t is constructed using these values:

$$\mathbb{P}(m_{t,i} = 1) = P_{\mu,i}^m, \quad \mathbb{P}(m_{t,i} = 0) = 1 - P_{\mu,i}^m.$$

B. Policy Gradient Algorithm for the TCN Model

For the TCN model, the weights are given by the weights of the kernel filters. Since the same kernel filters are applied at each time step, $\theta_t = \theta$, where θ denotes the weights of all the kernel filters. Thus, the vanilla policy gradient algorithm for this model is given by:

$$\theta \leftarrow \theta + \gamma_{\theta} \sum_t \delta_{t,r}^{\theta}.$$

Similarly the actor-critic algorithm AC- k is given by:

$$\theta \leftarrow \theta + \gamma_{\theta} \sum_t \delta_{t,k}^{\theta}.$$

V. RESULTS AND DISCUSSION

In this section we analyse the performance of the learning algorithm across different generation-consumption profiles. We also discuss specific market outcomes for each scenario to demonstrate how the learning algorithm matches. To evaluate the performance of the learning algorithm, the following online matching algorithms are considered:

- Match on Arrival (MA) algorithm: this algorithm matches the available renewable sources to the arriving customers. In case the renewable source is insufficient, the remaining customers would be matched to the grid supply.
- Match to the Highest (MH) algorithm: this algorithm matches the available renewable supply to the customers with the maximum willingness to pay value. Any remaining customer with an immediate deadline would be matched to the grid supply.
- Match to the Earliest Deadline (MED) algorithm: this algorithm matches the available renewable supply to the customers with the earliest deadlines. If the renewable supply is not sufficient enough, the customer with an immediate deadline would be matched to the grid supply.
- Learning Algorithm 1 (LA1): it denotes the vanilla policy gradient learning algorithm.
- Learning Algorithm 2 (LA2): it denotes the actor-critic algorithm of type AC-1.

The performance of the algorithms is compared in terms of the average social welfare across a certain number of epochs. The best hyper-parameters for TCN and Adam optimizer were selected by choosing the best parameters' combination across the scenario. The best hyper-parameters for the TCN model were identified to be 3 for the number of blocks, 4 for the number of filters, 3 for the filter size, 0.1 for the dropout factor and 4 for the dilation factor. Sigmoid function was utilized as the activation function for each output of TCN. We used the following values for the parameters of the ADAM algorithm: $\alpha = 0.75$, $\beta_1 = 0.9$, $\beta_2 = 0.999$, $\epsilon = 10^{-8}$, where α is the leaning rate and β_1 , β_2 are exponential decay rates for the

moment estimates. The best batch size is 80 and 120 for LA1 and 20 for LA2. The simulations are carried out on a sample power system with average load and renewable generation data for five different loading and generation scenarios as follows:

- Scenario 1: This scenario considers customers characterized by random short deadlines, with an average deadline of 4 time periods from arrival, and limited generation during the middle of the epoch. The average load request and renewable generation for this scenario are shown in Fig. 3-(a).
- Scenario 2: In this scenario, customers who arrive earlier have larger deadlines, while others who arrive during the middle of the epoch have shorter deadlines. The average load request and renewable generation are shown in Fig. 3-(b).
- Scenario 3: This scenario considers customers characterized by random large deadlines, with an average deadline of 8 time periods from arrival and excess generation during the middle of each epoch. The average load request and renewable generation for this scenario are shown in Fig. 3-(c).
- Scenario 4: This scenario considers customers characterized by fixed large deadlines of 8 time periods from arrival. The average load request and renewable generation for this scenario are shown in Fig. 3-(d).
- Scenario 5: This scenario is a hybrid of scenarios 1, 2 and 3, where on every $3k+1$ th epoch, $3k+2$ th epoch, $3(k+1)$ th epoch, $k \in \{0, 1, 2, \dots\}$, the load and generation and customer characteristics correspond to scenarios 1, 2 and 3 respectively.

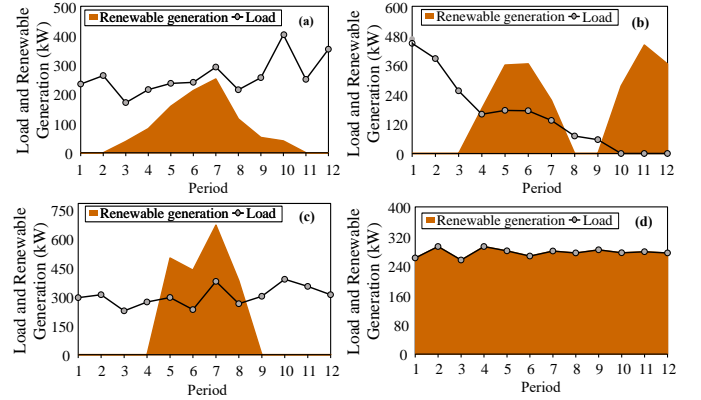


Fig. 3: Load request and renewable generation: (a) Scenario 1, (b) Scenario 2, (c) Scenario 3, (d) Scenario 4.

In the first four scenarios, LA2 is fed with load and generation data for 200 epochs, while LA1 and rest of the algorithms are fed with load and generation data for 800 epochs, generated using normal distribution with the average values shown in Fig. 3. The standard deviation to produce load and renewable generation profiles for scenarios 1-3 is equal to 15% of the average load and generation, shown in Fig. 3, while it is 50% of the average load and generation for scenario 4 to consider severe uncertainty in local load and generation. Every epoch includes 12-period load and generation samples and considering the number of epochs

discussed above, $(200 \text{ epochs}) \times (12 \text{ periods}) = 2400$ load and generation samples are utilized for LA2, while $(800 \text{ epochs}) \times (12 \text{ periods}) = 9600$ samples are utilized for LA1 and other algorithms in every scenario.

A. Numerical Results

The arriving load request and renewable generation are random in all the scenarios, but their mean level varies with time and differently in each scenario, as shown in Fig. 3. The average social welfare that is achieved by each algorithm for each scenario is shown in Table I. The results presented for the learning algorithms for each scenario are the best of the scores across the multiple runs. We find that the learning algorithms of both the types achieve the highest average social welfare across the scenarios. The learning algorithms LA1 and LA2 achieve an overall average of 170.8 and 173.1 while MH, MA and MED achieve an average score of 143.4, 151.8 and 132.4. Below, we discuss each of the scenarios in detail. We also note that the learning algorithms are the top performing algorithms for all the scenarios except scenario 1. While LA1 and LA2 achieve an almost similar score across the scenarios, the key difference is that the algorithm LA1 requires 800 epochs of data, while the algorithm LA2 requires just 200 epochs of data to achieve the same level of performance.

TABLE I: Average Social Welfare

Scenario \ Algorithm	MA	MH	MED	LA1	LA2
Scenario 1 (\$)	150.4	43	28.4	130.5	126.4
Scenario 2 (\$)	84.7	136.7	118.6	137.4	134.7
Scenario 3 (\$)	160	178.7	174.3	188.5	202.1
Scenario 4 (\$)	232.7	262.2	260.2	266.9	267.1
Scenario 5 (\$)	131.6	96.6	80.5	130.8	135.3
Average (all, \$)	151.8	143.4	132.4	170.8	173.1

1) *Scenario 1*: In this scenario the arriving customers have high criticality and short deadlines. The mean level of renewable generation varies and peaks during the middle of the epochs but is less than the arriving new load requests at all times (see Fig. 3). Hence, we can expect that waiting to serve the customers with delay will not be advantageous and can reduce the performance. Not surprisingly, we find that MA which matches on arrival achieves the highest social welfare. The average welfare achieved by each of the algorithms is shown in Table I. While MA achieves the highest average welfare of 150.4, the learning algorithms LA1 and LA2 are the second best at an average score of 130.5 and 126.4.

The matching by MA, MH and LA1 on a representative epoch is shown in Fig. 4. The figure shows how the learning algorithm matches after it learns. Here, we find that the learning algorithm was able to learn to match nearly on arrival.

2) *Scenario 2*: In this scenario customers are less critical, and some customers which arrive during the middle of the epoch have a smaller deadline and some others have a larger deadline. The renewable generation is in excess during the middle of the epoch and the later part of the epoch while it falls severely short of the arriving load request at other times (see Fig. 3). Hence the MA algorithm which matches on arrival can under-utilize the renewable generation both at the middle and the end of the epoch while in contrast MH can maximally

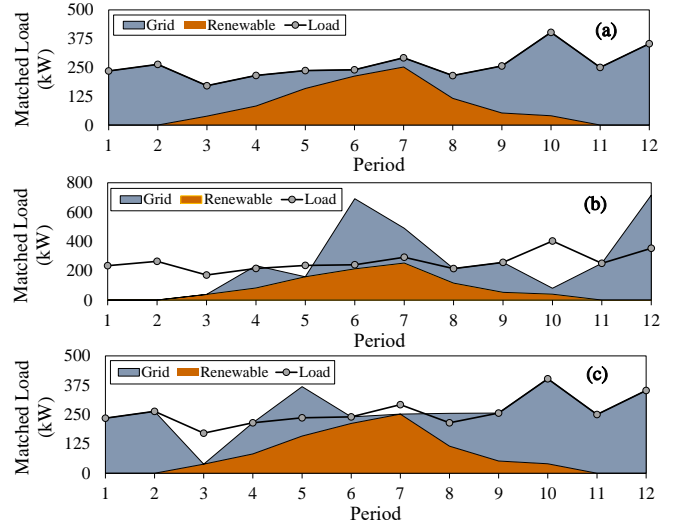


Fig. 4: Matching on a representative epoch (Scenario 1): (a) MA, (b) MH, (c) LA1.

utilize the renewable generation at both these times because it waits till it finds sufficient renewable generation. This is evident in Fig. 5, where matching by MA, MH and LA1 on a representative epoch is illustrated.

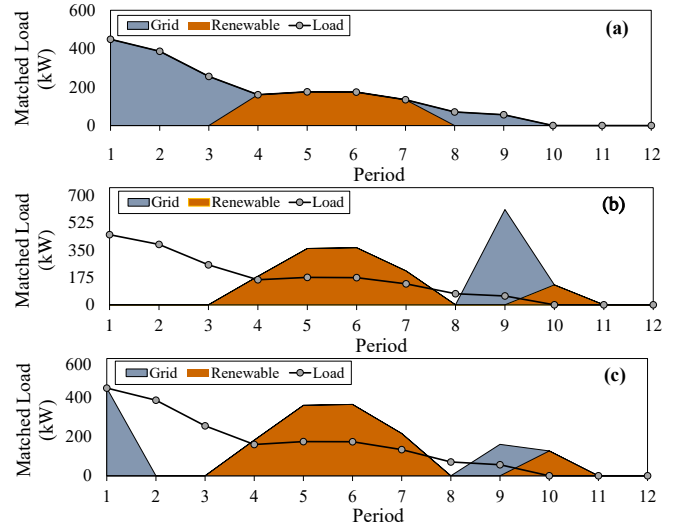


Fig. 5: Matching on a representative epoch (Scenario 2): (a) MA, (b) MH, (c) LA1.

The figure clearly shows that MH is able to leverage the customers' flexibility to match the renewable energy in excess of the arriving load request during the middle and the end of the epoch. As a result the majority of customers are matched to the renewable energy and the remaining critical ones are served by the grid. From the figure it is clear that the learning algorithm has learnt to delay the customers to utilize the renewable generation during the middle and end of the epoch. In addition, the learning algorithm does not delay all of the customers as MH does and matches some of the customers on arrival (see Fig 5). The average welfare achieved by the algorithms for this scenario is shown in Table I. We find

that the learning algorithm LA1 achieves the highest average welfare of 137.4, while MH achieves the second best average score of 136.7 closely followed by LA2 at 134.7.

3) *Scenario 3*: In this scenario, the difference from scenario 2 is the one peak in renewable generation instead of two. The matching algorithm can still gain from allowing the customers who arrive earlier and with longer deadlines to wait in order to match to the renewable generation during the peak. Therefore, not surprisingly we find that matching on arrival is not the best strategy for this scenario. The average welfare achieved by each of the algorithms for this scenario is shown in Table I. We find that the learning algorithms LA2 and LA1 achieve a high average score of 202.1 and 188.5 respectively.

The matching by MA, MED and LA1 on a representative epoch is illustrated in Fig. 6. The figure clearly shows that MA fails to leverage the customer’s flexibility when compared to MED and LA1 to maximize the matching to renewable energy. This is because MA matches the customers who arrive during the earlier part of the epoch to the grid on their arrival itself and does not wait. While the learning algorithm has learnt to wait to avail future renewable generation, unlike MED it matches some customers on arrival. As in scenario 2, this enables the learning algorithms to achieve a better score. Figure 7 shows how the average social welfare improves for the learning algorithm LA2 with the number of epochs of data. The figure clearly highlights the importance of the role played by the learning component of the proposed matching policy.

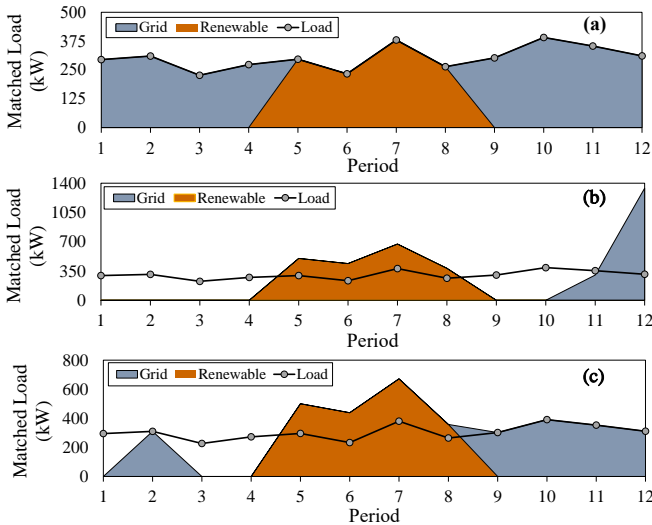


Fig. 6: Matching on a representative epoch (Scenario 3): (a) MA, (b) MED, (c) LA1.

4) *Scenario 4*: In contrast to the previous three scenarios, here the mean level of new load request and renewable generation are uniform throughout and nearly equal. The average welfare achieved by each of the algorithms for this scenario is shown in Table I. We find that the learning algorithms LA2 and LA1 achieve the highest average welfare of 267.1 and 266.9.

5) *Scenario 5*: This scenario is a hybrid of scenarios 1, 2 and 3. On every $3k + 1$ th epoch, $3k + 2$ th epoch, $3(k + 1)$ th epoch, $k \in \{0, 1, 2, \dots\}$, the load and renewable generation are

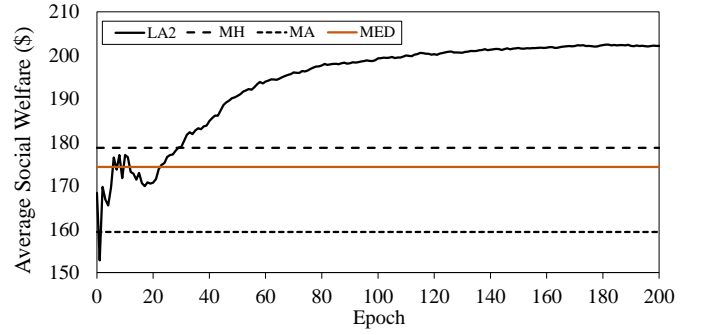


Fig. 7: Average social welfare for LA2 (Scenario 3).

different and correspond to scenarios 1, 2 and 3 respectively. While in previous scenarios the generation-consumption profiles are of the same type, in this scenario these profiles for each subsequent epoch differ. Figure 8 shows how the average social welfare improves for LA2 with the number of epochs of data. Table II shows the social welfare achieved by the various algorithms on the $3k + 1$ th, $3k + 2$ th, and $3(k + 1)$ th epoch for $k = 54$ and 63 . We find that MA, MH and MED fluctuate from being the best on one epoch to the worst performing on the other epoch. This is expected from the observations we made on these algorithms under the sections for scenarios 1, 2, and 3. Most importantly, we find that the learning algorithm LA2’s performance does not vary as much as the other three algorithms and is consistently among the top two performing algorithms on each individual epoch. From Table I we find that LA2 is the top performing algorithm overall with an average welfare of 135.3 across all the epochs.

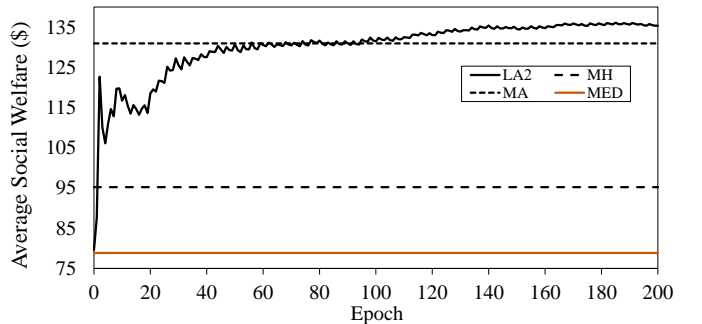


Fig. 8: Average social welfare for LA2 (Scenario 5).

TABLE II: Social welfare in Scenario 5

k	Epoch	Social Welfare (\$)			
		MA	MH	MED	LA2
54	163	165.3	68.1	47.5	113
	164	81.6	103	80.5	116.4
	165	161.0	194	194.2	216.5
	190	154.5	27	3.7	87.3
63	191	86.9	100.5	73.6	112.2
	192	157.2	183.7	184.8	214.6

VI. CONCLUSION

In this paper, a hybrid reinforcement learning framework is proposed for dynamic matching of flexible customers and

D-RES in power systems. The proposed hybrid learning framework is composed of a fixed rule-based function and a trainable component that can be directly trained by customer and D-RES data with no prior knowledge or expert supervision. The output from the proposed hybrid reinforcement learning framework is the matching policy for active customers and D-RES owners, which seeks to maximize social welfare in the matching market, respecting the servicing constraints of customers. Simulations are conducted on a test power system for different load and generation scenarios and the results show that the proposed hybrid reinforcement learning framework outperforms the other standard online matching heuristics in terms of leaning an effective matching policy that achieves higher social welfare in the matching market. The results shows that the hybrid reinforcement learning framework is much more effective than other algorithms in determining matching policy across various scenarios that differ in terms of load and generation profiles and customers servicing constraints. More specifically, it was found that the learning framework is the best performing algorithm across most of the scenarios, while the performance of other standard heuristics varies intensely based on the supply availability and customers characteristics, e.g., load request and criticality.

REFERENCES

- [1] Y. Parag and B. K. Sovacool, "Electricity market design for the prosumer era," *Nature Energy*, vol. 1, no. 4, pp. 1–6, 2016.
- [2] D. Muthirayan, D. Kalathil, S. Li, K. Poolla, and P. Varaiya, "Selling demand response using options," *IEEE Transactions on Smart Grid*, vol. 12, no. 1, pp. 279–288, 2020.
- [3] H. Rashidzadeh-Kermani, M. Vahedipour-Dahraie, M. Shafie-khah, and J. P. Catalao, "Stochastic programming model for scheduling demand response aggregators considering uncertain market prices and demands," *International Journal of Electrical Power & Energy Systems*, vol. 113, pp. 528–538, 2019.
- [4] S. Talari, M. Shafie-Khah, Y. Chen, W. Wei, P. D. Gaspar, and J. P. Catalao, "Real-time scheduling of demand response options considering the volatility of wind power generation," *IEEE Transactions on Sustainable Energy*, vol. 10, no. 4, pp. 1633–1643, 2018.
- [5] S. Talari, M. Shafie-Khah, F. Wang, J. Aghaei, and J. P. Catalao, "Optimal scheduling of demand response in pre-emptive markets based on stochastic bilevel programming method," *IEEE Transactions on Industrial Electronics*, vol. 66, no. 2, pp. 1453–1464, 2017.
- [6] E. Heydarian-Forushani, M. Golshan, M. Moghaddam, M. Shafie-Khah, and J. Catalão, "Robust scheduling of variable wind generation by coordination of bulk energy storages and demand response," *Energy Conversion and Management*, vol. 106, pp. 941–950, 2015.
- [7] M. Parvania, M. Fotuhi-Firuzabad, and M. Shahidehpour, "Iso's optimal strategies for scheduling the hourly demand response in day-ahead markets," *IEEE Transactions on Power Systems*, vol. 29, no. 6, pp. 2636–2645, 2014.
- [8] R. Tyagi, J. W. Black, and J. Petersen, "Optimal scheduling of demand response events using options valuation methods," in *2011 IEEE Power and Energy Society General Meeting*. IEEE, 2011, pp. 1–5.
- [9] R. M. Karp, U. V. Vazirani, and V. V. Vazirani, "An optimal algorithm for on-line bipartite matching," in *Proceedings of the twenty-second annual ACM symposium on Theory of computing*. ACM, 1990, pp. 352–358.
- [10] B. Kalyanasundaram and K. Pruhs, "Online weighted matching," *Journal of Algorithms*, vol. 14, no. 3, pp. 478–488, 1993.
- [11] A. Mehta, A. Saberi, U. Vazirani, and V. Vazirani, "Adwords and generalized on-line matching," in *46th Annual IEEE Symposium on Foundations of Computer Science (FOCS'05)*. IEEE, 2005, pp. 264–273.
- [12] P. Jaillet and X. Lu, "Online stochastic matching: New algorithms with better bounds," *Mathematics of Operations Research*, vol. 39, no. 3, pp. 624–646, 2013.
- [13] A. Blum, T. Sandholm, and M. Zinkevich, "Online algorithms for market clearing," *Journal of the ACM (JACM)*, vol. 53, no. 5, pp. 845–879, 2006.
- [14] D. Muthirayan, M. Parvania, and P. P. Khargonekar, "Online algorithms for dynamic matching markets in power distribution systems," *IEEE Control Systems Letters*, vol. 5, no. 3, pp. 995–1000, 2020.
- [15] G. Dulac-Arnold, D. Mankowitz, and T. Hester, "Challenges of real-world reinforcement learning," *arXiv preprint arXiv:1904.12901*, 2019.
- [16] A. Parisio, E. Rikos, and L. Glielmo, "A model predictive control approach to microgrid operation optimization," *IEEE Transactions on Control Systems Technology*, vol. 22, no. 5, pp. 1813–1827, 2014.
- [17] W. Shi, N. Li, C.-C. Chu, and R. Gadh, "Real-time energy management in microgrids," *IEEE Transactions on Smart Grid*, vol. 8, no. 1, pp. 228–238, 2015.
- [18] R. Khatami, M. Heidarifar, M. Parvania, and P. Khargonekar, "Scheduling and pricing of load flexibility in power systems," *IEEE Journal of Selected Topics in Signal Processing*, vol. 12, no. 4, pp. 645–656, 2018.
- [19] R. Khatami, M. Parvania, and A. Bagherinezhad, "Continuous-time model predictive control for real-time flexibility scheduling of plugin electric vehicles," *IFAC-PapersOnLine*, vol. 51, no. 28, pp. 498–503, 2018.
- [20] K. Oikonomou, M. Parvania, and R. Khatami, "Deliverable energy flexibility scheduling for active distribution networks," *IEEE Transactions on Smart Grid*, vol. 11, no. 1, pp. 655–664, 2019.
- [21] B. Li, T. Chen, X. Wang, and G. B. Giannakis, "Real-time energy management in microgrids with reduced battery capacity requirements," *IEEE Transactions on Smart Grid*, vol. 10, no. 2, pp. 1928–1938, 2017.
- [22] S. Sun, M. Dong, and B. Liang, "Distributed real-time power balancing in renewable-integrated power grids with storage and flexible loads," *IEEE Transactions on Smart Grid*, vol. 7, no. 5, pp. 2337–2349, 2015.
- [23] P. Ströhle and C. M. Flath, "Local matching of flexible load in smart grids," *European Journal of Operational Research*, vol. 253, no. 3, pp. 811–824, 2016.
- [24] Y. Du, J. Wu, S. Li, C. Long, and I. C. Paschalidis, "Distributed mpc for coordinated energy efficiency utilization in microgrid systems," *IEEE Transactions on Smart Grid*, vol. 10, no. 2, pp. 1781–1790, 2017.
- [25] R. S. Sutton and A. G. Barto, *Reinforcement learning: An introduction*. MIT press, 2018.
- [26] F. L. Lewis and D. Vrabie, "Reinforcement learning and adaptive dynamic programming for feedback control," *IEEE circuits and systems magazine*, vol. 9, no. 3, pp. 32–50, 2009.
- [27] D. P. Bertsekas, *Abstract dynamic programming*. Athena Scientific, 2018.
- [28] V. Mnih, K. Kavukcuoglu, D. Silver, A. A. Rusu, J. Veness, M. G. Bellemare, A. Graves, M. Riedmiller, A. K. Fidjeland, G. Ostrovski et al., "Human-level control through deep reinforcement learning," *nature*, vol. 518, no. 7540, pp. 529–533, 2015.
- [29] D. Silver, J. Schrittwieser, K. Simonyan, I. Antonoglou, A. Huang, A. Guez, T. Hubert, L. Baker, M. Lai, A. Bolton et al., "Mastering the game of go without human knowledge," *nature*, vol. 550, no. 7676, pp. 354–359, 2017.
- [30] T. P. Lillicrap, J. J. Hunt, A. Pritzel, N. Heess, T. Erez, Y. Tassa, D. Silver, and D. Wierstra, "Continuous control with deep reinforcement learning," *arXiv preprint arXiv:1509.02971*, 2015.
- [31] J. Schulman, S. Levine, P. Abbeel, M. Jordan, and P. Moritz, "Trust region policy optimization," in *International conference on machine learning*. PMLR, 2015, pp. 1889–1897.
- [32] H. Hasselt, "Double q-learning," *Advances in neural information processing systems*, vol. 23, pp. 2613–2621, 2010.
- [33] J. Schulman, P. Moritz, S. Levine, M. Jordan, and P. Abbeel, "High-dimensional continuous control using generalized advantage estimation," *arXiv preprint arXiv:1506.02438*, 2015.
- [34] J. Schulman, F. Wolski, P. Dhariwal, A. Radford, and O. Klimov, "Proximal policy optimization algorithms," *arXiv preprint arXiv:1707.06347*, 2017.
- [35] V. Mnih, A. P. Badia, M. Mirza, A. Graves, T. Lillicrap, T. Harley, D. Silver, and K. Kavukcuoglu, "Asynchronous methods for deep reinforcement learning," in *International conference on machine learning*. PMLR, 2016, pp. 1928–1937.
- [36] Z. Wang, V. Bapst, N. Heess, V. Mnih, R. Munos, K. Kavukcuoglu, and N. de Freitas, "Sample efficient actor-critic with experience replay," *arXiv preprint arXiv:1611.01224*, 2016.
- [37] D. P. Kingma and J. Ba, "Adam: A method for stochastic optimization," *arXiv preprint arXiv:1412.6980*, 2014.
- [38] S. Bai, J. Z. Kolter, and V. Koltun, "An empirical evaluation of generic convolutional and recurrent networks for sequence modeling," *arXiv preprint arXiv:1803.01271*, 2018.
- [39] D. Ulyanov, A. Vedaldi, and V. Lempitsky, "Instance normalization: The missing ingredient for fast stylization," *arXiv preprint arXiv:1607.08022*, 2016.

- [40] N. Srivastava, G. Hinton, A. Krizhevsky, I. Sutskever, and R. Salakhutdinov, "Dropout: a simple way to prevent neural networks from overfitting," *The journal of machine learning research*, vol. 15, no. 1, pp. 1929–1958, 2014.